Characterization of the Degradation Process of Lithium-ion Batteries when Discharged at Different Current Rates

Aramis Perez[1], Vanessa Quintero[1,2], Francisco Jaramillo[1], Heraldo Rozas[1], Diego Jimenez[1], Marcos Orchard[1] and Rodrigo Moreno[1,3]

Abstract

The use of energy storage devices, such as lithium-ion (Li-ion) batteries, has become popular in many different domains and applications. Hence, it is relatively easy to find literature associated with problems of battery state-of-charge estimation and energy autonomy prognostics. Despite this fact, the characterization of battery degradation processes is still a matter of ongoing research. Indeed, most battery degradation models solely consider operation under nominal (or strictly controlled) conditions, although actual operating profiles (including discharge current) may differ significantly from those. In this context, this article proposes a Li-ion battery degradation model that incorporates the impact of arbitrary discharge currents. Also, the proposed model, initially calibrated through data reported for a specific Li-ion battery type, can characterize degradation curves for other Li-ion batteries. Two case studies have been carried out to validate the proposed model, initially calibrated by using data from a Sony battery. The first case study uses our own experimental data obtained for a Panasonic Li-ion cell, which was cycled and degraded at high current rates. The second case study considers the analysis of two public data sets available at the Prognostics Center of Excellence of NASA Ames Research Center website, for batteries cycled using nominal and 2-C (twice the nominal) discharge currents. Results show that the proposed model can characterize degradation processes properly, even when cycles are subject to different discharge currents and for batteries not manufactured by Sony (whose data was used for the initial calibration).

Introduction

Carbon dioxide emissions reduction through increased participation of renewables and new innovative, smart grid technologies such as Energy Storage Devices (ESDs) in the electricity sector is of utmost importance due to global warming (1) (2). As the number of applications powered by ESDs grows by the day, the need to understand their performance under various operating conditions increases (1) (3). Li-ion batteries, in particular, are the preferred choice for ESDs in many applications such as electromobility, frequency control in the electricity system, etc. (4) (5). Several research efforts have focused on the study of Li-ion battery State-of-Charge (SOC), a parameter that is related to the short-term energy usage and availability (2) (4). Notwithstanding the above, the characterization of battery degradation processes in the longer term is still a matter of ongoing research. Battery degradation is typically characterized by the State-of-Health (SOH) (1) (6). Both the SOC and the SOH cannot be measured directly, and thus they must be estimated through other variables (6).

A critical matter in this paper is how the usage of a given Li-ion battery and the environment in which this is immerse affect its SOH and Remaining Useful Life (RUL) (5). Most studies assume that batteries undergo nominal operating conditions. However, actual battery usage may differ significantly from those conditions due to, for example: temperature variations, high discharge current rates, and different SOC swing ranges per cycle (6) (7).

To overcome some of these difficulties, at least in terms of the characterization of battery SOH, we propose a novel model that incorporates the discharge current as a feature that directly affects the degradation process of Li-ion batteries. Also, the proposed model, initially calibrated through data reported for a specific Li-ion battery type, can characterize degradation curves for other Li-ion batteries. Two case studies have been used to validate the proposed model.

Theoretical Background

Degradation and ageing are processes that clearly affect Li-ion batteries. According to (8) Li-ion batteries are complex systems where capacity and power fading processes may

[1] Department of Electrical Engineering, University of Chile, CL.
[2] Faculty of Electrical Engineering, Universidad Tecnológica de Panamá, PA.
[3] Department of Electrical and Electronic Engineering, Imperial College London, UK.

Corresponding author:
Aramis Perez, Department of Electrical Engineering, University of Chile, Av. Tupper 2007, Santiago, Chile
Email: aramis.perez@ing.uchile.cl

be caused by multiple reasons such as: temperature, cycling rate, storing and operating conditions to mention a few (6). Moreover, the same authors found that variable operating conditions may enhance damages on several components of the battery. For example, operating a battery at high temperatures causes the decomposition of the electrolyte, while high cycling rates might cause a reduction of the contact area between the cations and the electrolyte (7).

Different factors have a direct impact on the overall performance of the ESD; while some factors can be controlled by the user, others cannot. The C-rate is an important parameter to consider in the characterization of battery usage cycles (9). The C-rate is a measure of the rate at which a battery is discharged with respect to its nominal capacity (a 1-C rate means that the discharge current will discharge the entire battery in 1 hour). Other aspects to be considered are the type of discharge-charge cycle, battery temperature, conditions of how the battery is stored and manipulated, and pressure (1) (4). There is evidence that relates the atmospheric temperature to the performance of a battery (10). Although differences in the delivered energy (i.e. energy capacity) can be explained due to changes of the temperature through different equations and models (11) (12) (13) (14), there is less information regarding the evolution of degradation processes when batteries undergo different discharge current rates. In other words, the majority of existing degradation models are solely validated at nominal discharge currents.

Degradation Models

A proper characterization of the battery SOC and SOH may be critical in the development of an intelligent Battery Management System (BMS), since knowledge on the state of battery pack allows adequate decision making for both immediate and future use (15). The scientic community has not yet agreed on a unique procedure to estimate the SOH, mainly due to the level of complexity of variables that affect the process (16) (17). Regardless of this fact, different types of models for battery SOH estimation have been proposed to this date. For example, authors in (17) classify methods for SOH estimation in two categories: either open-loop or closed-loop. The former use experimental data as well as previous knowledge of the operating conditions. The latter category intends to describe the behavior of the battery (equivalent-circuit models or electrochemical models).

In (16) the authors classified the model as experimental or adaptive. Experimental models are based on a combination of historical battery cycling data and expert knowledge on a specific battery to determine the parameters that affect its lifespan, including, for example, models based on Electrochemical Impedance Spectroscopy (EIS) analysis, Support Vector Machines (SVM), Coulomb-counting, data maps, and some probabilistic models (16). The main advantage of these models is that the calculation of relevant parameters can be undertaken in a fast manner, while the main disadvantage is that the performance might not be as good since the battery behavior changes in time.

On the other hand, adaptive models focus on adjusting the parameters that are sensitive to the battery degradation as time goes on. As these models process data acquired in real-time, they can be very versatile, allowing to adjust

a determined model structure to any battery type or age. However, these models require a high computational cost, increasing their difficulty for on-line implementation (16). Kalman filters, artificial neural networks, fuzzy logic, least squares, among others are some examples of these types of models.

The SOH estimation is a field of great interest for the scientific community, where the efforts have been focused on the modeling of different battery aging mechanisms (17). An example of this is the work presented in (18), where a general model for the estimation of the SOC and SOH was proposed. The results were demonstrated on a nickel manganese cobalt pouch cell and were extended to any type of cell chemistry. However, in practice, the proposed model depends on many unknown parameters, making it difficult to simulate or implement for a general case. EIS-based models are accurate for the analysis of battery degradation processes. However, EIS-based models require expensive equipment to measure the battery internal impedance, and the measurement procedure has to be performed off-line, meaning that the battery has to be disconnected from the load while it is being analyzed. Although the EIS analysis does not give a percentage value of the degraded capacity of the battery, the resulting information is very helpful: the EIS provides a Nyquist plot of the internal impedance of the battery at a wide range of frequencies (19).

In (20), the authors propose a model that controls the battery Depth of Discharge (DoD) by manipulating the discharge time, and where the final discharge voltage is estimated as a function of the cycle number. Similarly, a generalized charge-discharge model based on the loss of the active lithium ions due to electrochemical solvent reduction at anode/electrolyte interface, is presented in (21). These works demonstrated that the way an ESD is charged and discharged also has an impact on its ageing. In the same line in (22), the authors verified that higher C-rates lead to less available cycles, meaning that the degradation process is accelerated.

The degradation caused in the ESD affects the capability of storing energy. In others words, as the ESD degrades, the amount of energy that can be stored decreases. In this regard, one of the simplest battery degradation models is based on the concept of Coulombic efficiency, denoted through the greek letter η (23). This efficiency is defined as the capability to store energy from one cycle to another (24). In other words, it represents the rate between the maximum energy capacity that can be stored in one cycle when compared to the maximum energy capacity stored on the previous cycle. Depending on the type of model there can be one efficiency for charging and a different one for discharging. This efficiency is affected by the DoD and the temperature at which batteries are stored and operated. In (25), the Coulombic efficiency is also incorporated in the model and the End of Life (EoL) can be predicted using a particle filter framework.

Battery capacity degradation curves may offer either convex or concave shapes (26). Based on this fact, some researchers have proposed a model for capacity degradation that incorporates two terms based on natural logarithm functions, which fits accurately when the degradation curve has a concave shape. Unfortunately, this model structure is

less efficient in fitting experimental data that shows a convex shape, which is the case that was verified in our experiments.

A different approach was performed by (27). In this case, the authors propose the concept of Sample Entropy used as an input feature to train two systems: one based on SVM and the other one based on Relevance Vector Machines (RVM). The method proposed in (27) attempts to predict the SOH of the battery using the nominal capacity at different time instants. Since this method includes a learning algorithm, it requires to be validated before proper implementation.

In (28), a SOH degradation model is proposed considering data from the charging state. The features considered from the charging data were the length of Constant Current Charge Time (CCCT) and the Constant Voltage Charge Time (CVCT). This model is able to predict that, as the battery degrades, the CVCT will increase and the CCCT will decrease. In (28), an experimental procedure was performed on three different prismatic batteries. The other two variables considered in the model are the internal resistance and the capacity.

As the internal resistance plays a key role in the SOH degradation, different models have been developed in order to estimate its value. This task is not easy due to the nonlinearities present due to the internal chemical processes. In (29) a frequency-based method to determine the internal impedance is presented. In this case, the authors prove that there is a direct linear relationship between the internal impedance and the SOH, in the frequency domain. A different point of view is presented in (30). The authors propose a SOH degradation model based on Ampere-hour throughput. This is defined as the current throughput and represents the energy delivered or stored in the battery. The Ampere-hour throughput can be described as a function of the open circuit voltage of the battery, and the intention is to use unique characteristics of the throughput in order to estimate the SOH while the battery ages. In this approach, the throughput function is generated by using constant current charge and discharge profiles, proposing a quadratic fit to obtain the SOH value.

An analytical approach based on recursive least squares was proposed in (31). The authors use this technique to determine certain parameters to estimate in real time the SOC and SOH of a Li-ion battery used for an electric vehicle. The discharge profiles are designed to meet with different driving patterns, for instance representing an agressive driver o a passive driver. In this experiment, the temperature is a controlled variable due to the battery cycle used in the process. The SOH degradation model is based on the online identification of the internal resistance.

When performing state-space modeling for remaining useful life prediction, it is important to consider the effect that the noise variances can cause if they are not properly dimensioned. Typically their values are considered to be fixed, although if their value is too small, it will take a while until the initial guess states approach the true states. Moreover, if the noise variance is too large, state-space filtering can diverge (5). In (5), the authors propose an efficient method for battery RUL prediction that is capable of updating the noise variances when new measurements are available.

Finally, reference (32) presents a Prognostics and Health Management (PHM) based empirical model that analyzes the RUL of the Li-ion batteries. The model parameters are initialized through a Dempster-Shafer Theory approach, and later updated through Bayesian Monte Carlo techniques to manage the uncertainty of the degradation process.

C-rate models

One of the Li-ion battery degradation models that explicitly includes the C-rate was proposed in (33). In this case, the authors study the performance of the vehicle-to-grid (V2G) interaction through a mathematical model of the battery, where the model parameters are adjusted through genetic algorithms. The model is based on an electric equivalent and a decreasing capacity approach of the processed energy at different C-rates. Then, the results are compared to the original datasheet in order to obtain the capacity degradation. This degradation is reported to be proportional to the applied C-rate.

In (34), the authors propose an empirical model for the capacity reduction in electric vehicles under different operating conditions. The main idea is to optimize the lifespan of the battery by maintaining a low SOC, avoiding sudden temperature changes and by charging the battery to a certain SOC level that is just enough for the next trip. However, the latter is difficult to undertake in practice since, in a more realistic scenario, it is not always possible to accurately plan or know the next trip. Also, this method does not inform about the degradation of the battery in terms of the number of cycles during the lifespan. Another model is proposed in (35), where the authors present a model that relates the increase in degradation with the increase in C-rate, analyzing different temperature conditions. The proposal corresponds to a mathematical pseudo-bidimensional model that integrates a solid electrolyte interface growth model.

A discharge-rate-dependent model is proposed on (36). This effort consisted of an experiment that discharged the battery at four different current rates (0.5-C, 1-C, 3-C and 5-C), with intermediate charges at the same rate (1-C). Every time this sequence was repeated, the authors defined a four-cycle rotation for modeling purposes. In this case, the model is based on an exponential function obtained after fitting the available capacity degradation data of three batteries, and by using the amplitude and slope of the exponential function it is possible to correlate them with the different discharge current rates. Using their proposed model, these authors also perform remaining useful life prognosis on a fourth battery that was discharged and charged in the same manner as the original three batteries.

All these efforts represent important steps towards the characterization of the battery SOH as a function the utilization or usage profile of the ESD. However, their application on SOH prognostic approaches, where the main objective is to predict the moment in which the device has to be replaced, is still limited. Our proposal aims to provide the means to improve our prediction capabilities in terms of the evolution of the battery SOH as a function of future discharge current rates.

Capacity Degradation Data

This research uses data provided in (22), where the authors cycled a Sony US18650 1.4 Ah Li-ion battery using different discharge rates (1-C, 2-C and 3-C), at a controlled ambient temperature. After 300 cycles, battery capacities were reduced by 9.5%, 13.2% and 16.9% when using 1-C, 2-C and 3-C, respectively. Figure 1 shows the capacity fade results measured every 50 cycles (please note that actual measurements are connected by straight lines in the figure). The same information in Figure 1 can be used to build the associated capacity degradation curve (see Figure 2). Note that the trend associated with the capacity degradation process follows a convex shape.
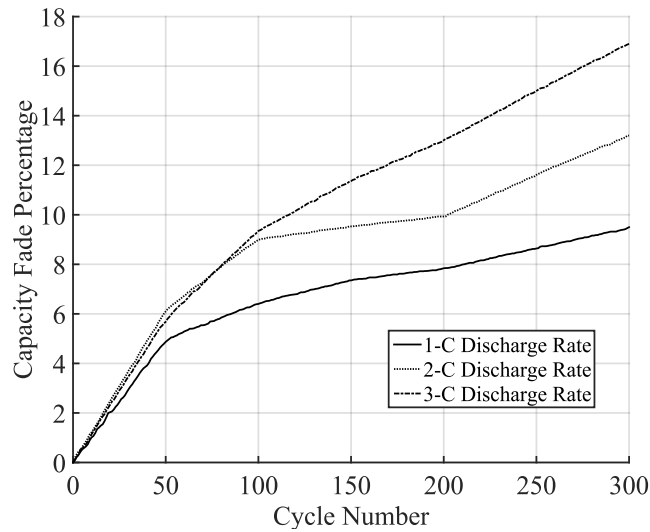
Figure 1. Capacity fade measured every 50 cycles for different discharge currents. Adapted from (22).
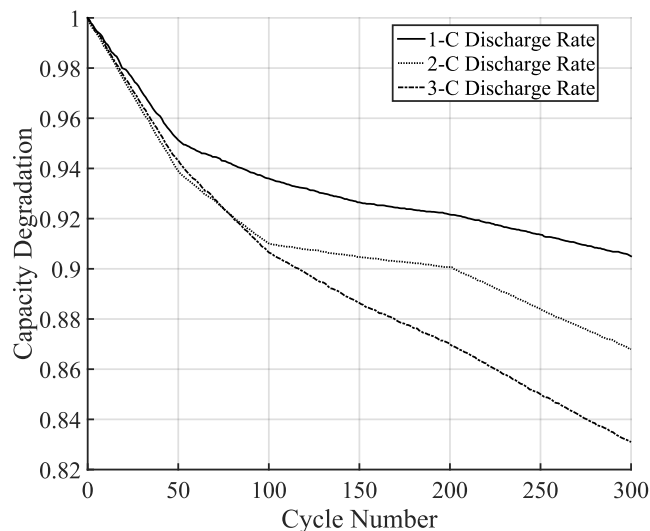
Figure 2. Capacity degradation process for different discharge currents.

Capacity fade curves are used by manufacturers to illustrate the battery degradation on datasheets. Consider for example Figure 3, which depicts an image adapted from the official datasheet of the Panasonic NCR18650B Li-ion battery. Typically, capacity fade curves are built by using data from batteries that are discharged under controlled conditions (DoD, temperature, charging and discharging current rates). Although this information is helpful to compare the expected performance of batteries from different brands, it does not suffice to characterize the impact of higher current rates.
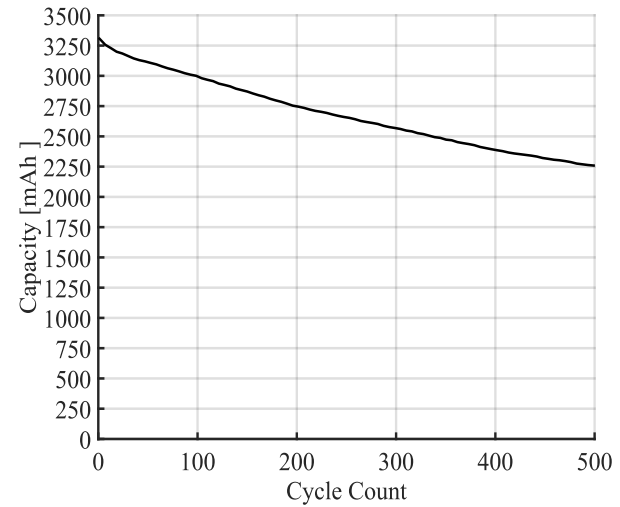

Figure 3. Panasonic NCR18650B Li-ion battery lifespan characteristics. Adapted from the original datasheet.

As it was previously mentioned, degradation processes can be characterized through the concept of Coulombic efficiency. However, in this research, the intention is to include the C-rate as a variable of the degradation process. It is interesting to note that all degradation curves shown in Figure 2 exhibit exponential decay regardless of the associated C-rate. We followed this intuition and used the Curve Fitting Tool from Matlab® to fit a two-summand exponential expression, $f(t) = ae^{bt} + ce^{dt}$, to actual degradation data. Figure 4 shows the measured data and the corresponding fitted curve.
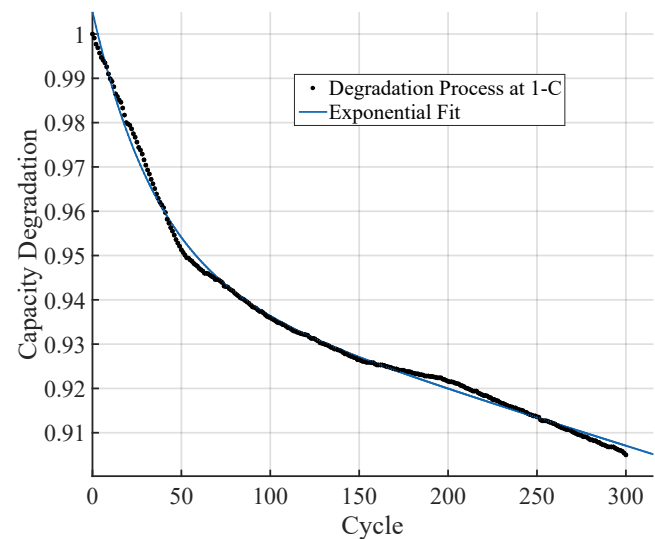

Figure 4. Capacity degradation process and fitted curve at 1-C.

Figures 5 and 6 show the individual contribution of each summand in $ae^{bt} + ce^{dt}$. It can be noted that each summand exhibits a different trend. On the one hand, the first summand represents a contribution that decreases exponentially in

time, and where differences among diverse discharge rates are almost negligible after 200 cycles of operation. In addition, the value of the first summand can be neglected in the long term, while it represents about 7% of the total battery capacity during the first operating cycles. Note that the second summand represents an affine function of time, where the slope depends on the battery discharge current. This suggests that this component could be used for better characterization of the degradation trend. Also, it can be stated that while the first summand has a major impact in the short term the second summand has a major impact in the long term.
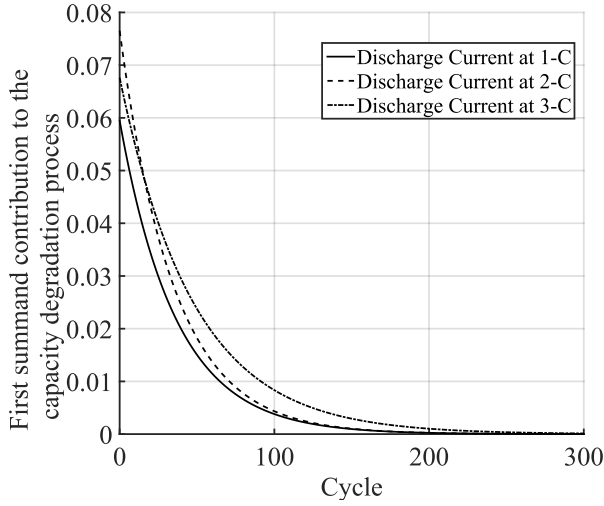
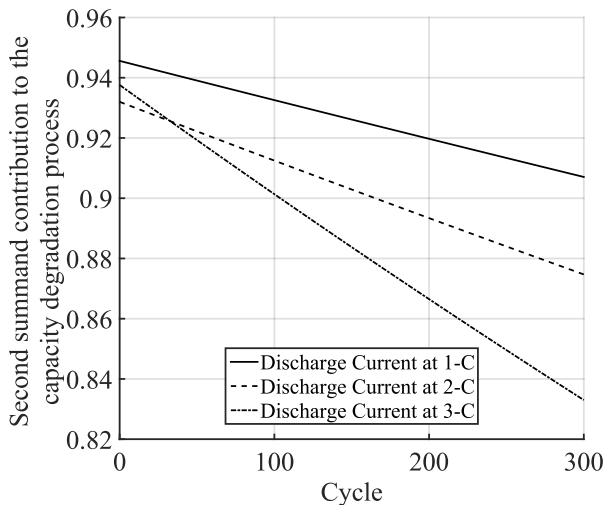**Figure 5.** First summand contribution to the capacity degradation process.

Figure 6. Second summand contribution to the capacity degradation process.

Proposed SOH Degradation Model

Given that the degradation process can be modeled as the sum of exponential functions in time, a two-state-space equation model is proposed:

$$\dot{\bar{x}}(t) = \begin{pmatrix} b & 0 \\ 0 & d \end{pmatrix} \bar{x}(t)$$
$$y(t) = \begin{pmatrix} a & c \end{pmatrix} \bar{x}(t)$$

Equivalently, the continuous state-space model can be rewritten in the following discrete-time form (sampling time equals to 1 cycle):

$$\begin{cases} x_1(k+1) = & e^b x_1(k) \\ x_2(k+1) = & e^d x_2(k) \end{cases} \tag{1}$$

$$y(k) = a x_1(k) + c x_2(k) \tag{2}$$

The values for the coefficients (mean value and the 95% confidence bounds) obtained through the Curve Fitting Tool of Matlab® are shown in Table 1.

Figure 7 summarizes the contributions of each summand to $y(k)$ for three discharge cases, where the mean values of the coefficients have been used. It is known that when a battery is new, its SOH will be 100% (or, equivalently, $y(0) = 1$). The procedure to determine initial conditions for the system states has to consider this fact. In this regard, we propose a step-by-step procedure to compute $x_1(0)$ and $x_2(0)$.
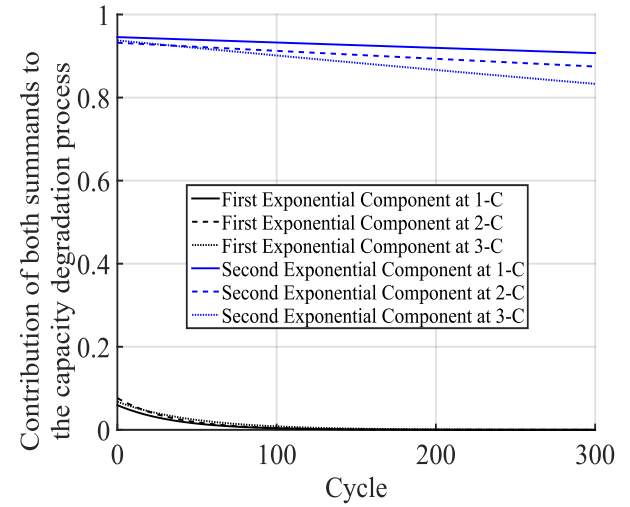

Figure 7. First and second summand contributions to the capacity degradation process at different C-rates.

As mentioned previously, the second summand represents the major long-term contribution in the total value of $y(k)$. For this reason, the procedure prioritizes a reasonable initial condition for the state x_2:

1. Determine the values of coefficients a, b, c, and d by using a fitting tool.
2. Assign $x_2(0) := 1$.
3. Solve for $x_1(0)$, such that $y(0) = 1$.

In the example previously described, we have:

$$y(k) = a x_1(k) + c x_2(k)$$
$$y(0) = 0.06108 x_1(0) + 0.946 x_2(0)$$

Table 1. Mean value and confidence bounds of the model coefficients.

Coefficient	Parameter	1-C	2-C	3-C
a	Mean Value	0.06108	0.07653	0.06763
	Confidence bounds	(0.06084, 0.06132)	(0.07371, 0.07965)	(0.06588, 0.06937)
b	Mean Value	-0.02905	-0.02896	-0.02093
	Confidence bounds	(-0.02931, -0.02879)	(-0.03165, -0.02627)	(-0.02203, -0.01984)
c	Mean Value	0.946	0.932	0.9376
	Confidence bounds	(0.9457, 0.9462)	(0.9292, 0.9349)	(0.9357, 0.9395)
d	Mean Value	-0.0001406	-0.0002115	-0.0003943
	Confidence bounds	(-0.0001416, -0.0001395)	(-0.000225, -0.000198)	(-0.0004026, -0.000386)

Fixing the value of $x_2(0)$ equal to 1, and knowing that $y(0)$ is equal to 1, then

$$1 = 0.06108x_1(0) + 0.946 \cdot 1$$
$$x_1(0) = 0.8841.$$

Now that the procedure for establishing the initial conditions has been explained, we verify the performance of the SOH model. Given that the curve fitting tool generates mean values and confidence bounds for each model parameter a, b, c, and d (see Table 1), we proceed to generate 10 sets of random coefficients, assign different initial conditions to each resulting model, and compare the evolution in time of the SOH model with actual measured data obtained from (22) (see Figure 8).
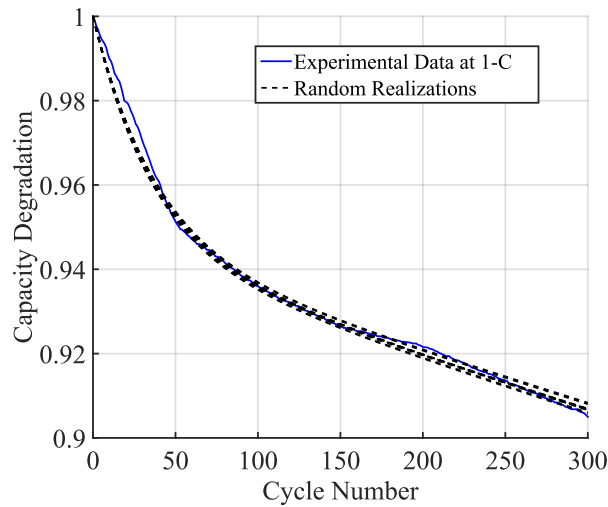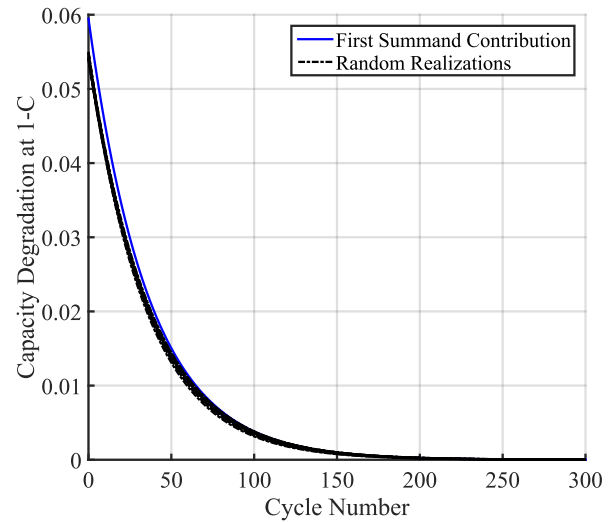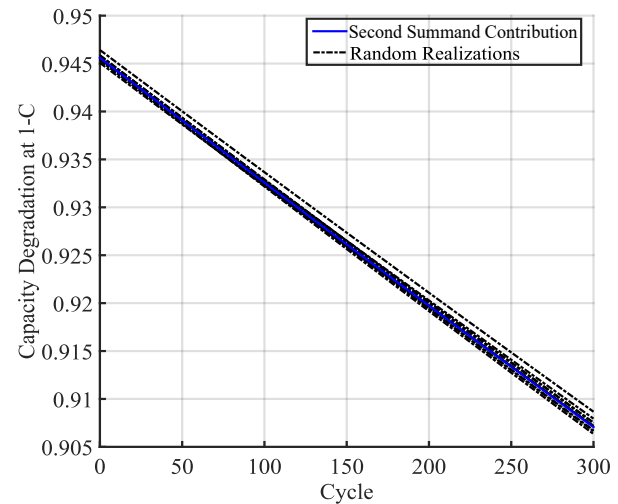

Figure 9. Comparison among first original summand and ten realizations.

Figure 8. Proposed model generated with random coefficients.

Figure 10. Comparison among second original summand and ten realizations.

Figure 9 compares the contribution of the first summand $ax_1(k)$ for each realization of random coefficients (and the corresponding set of initial conditions $x_1(0)$ and $x_2(0)$). Note that after nearly 50 cycles, all 10 realizations exhibit basically the same behaviour.

In case of the second summand, $cx_2(k)$, and since the initial condition is always set to $x_2(0) = 1$, we observe a greater contribution to the overall characterization of the battery SOH in time (see Figure 10).

Coefficient Analysis

As explained before, the model is composed of two-state-space equations and the corresponding observation

equation. A total of four coefficients are needed, all of them estimated via a curve fitting procedure. This section analyzes the model, in terms of the relationships between these parameters and the operating conditions at each discharge cycle.

Coefficient a: There is no clear pattern that could relate the values of this parameter and the battery discharge

current. There is no overlap among confidence intervals. An interesting issue is that the mean value in the 2-C case is the highest among the three cases. In this regard, there is no evidence of a monotonic relationship between parameter values and discharge current rates.

Coefficient b: In this case, it is possible to note that, for both the 1-C and 2-C cases, the confidence bounds are reasonably similar. Furthermore, it can be noted that the mean value of the 2-C case is within the confidence bounds of the 1-C case and vice-versa. This situation suggests that these two cases can be merged into just one confidence interval. It is suggested to consider 3-C battery discharges as a separate case, given that that mean value of the parameter is about 30% less than in the other cases.

Coefficient c: This coefficient is closely related to the initial value of the second summand of the observation equation, $cx_2(0)$. When comparing mean values and confidence intervals of 2-C and 3-C discharges, differences are small. However, it is recommended to assume a dependency between the parameter value and the battery discharge current in the implementation of the estimation approach.

Coefficient d: This coefficient has a major effect on the characterization of the degradation process since it is associated with the slope of the second summand in the observation equation, $cx_2(k)$. In this case, the mean values and confidence bounds are separated for each battery operating condition and, moreover, parameter values have a monotonic relationship with respect to the discharge current.

An interesting fact associated with the mean value of coefficient d is that the 1-C case is practically scaled to the nominal capacity of the battery (1.4 Ah). Table 2 summarizes the mean values of the three cases in terms of the nominal capacity. Another fact is that the mean values can be fitted through an exponential curve as shown in Figure 11.

Table 2. Mean value and confidence bounds of coefficient d at various discharge currents (Values must be multiplied by $10^{(-4)}$).

Parameter	Mean Value	Confidence Values
1-C	$-1 \cdot C_{nom}$	$(-1.01, -0.996) \cdot C_{nom}$
2-C	$-1.5 \cdot C_{nom}$	$(-1.6, -1.4) \cdot C_{nom}$
3-C	$-2.8 \cdot C_{nom}$	$(-2.88, -2.76) \cdot C_{nom}$

Indeed, from collected evidence, we have found that it is possible to find an exponential relationship between values of the coefficient d (in the proposed SOH degradation model) and the battery discharge current rate. This relationship can be characterized by the expression $y(\gamma) = \alpha e^{(\beta \cdot (\gamma)^2)}$, where γ is used to represent the C-rate and $y(\gamma)$ is a multiplier used to obtain the coefficient d of the model. Thus, we finally obtain a C-rate dependent model for SOH degradation over time, defined by state equations (1)-(2), and where:

$$d_1(C_{rate}) = \alpha e^{(\beta \cdot (C_{rate})^2)}. \quad (3)$$

The mean value and the confidence bounds of α and β are shown in Table 3. In this case, the obtained R^2 was 0.9997 (that reflects the goodness of the fitted function).
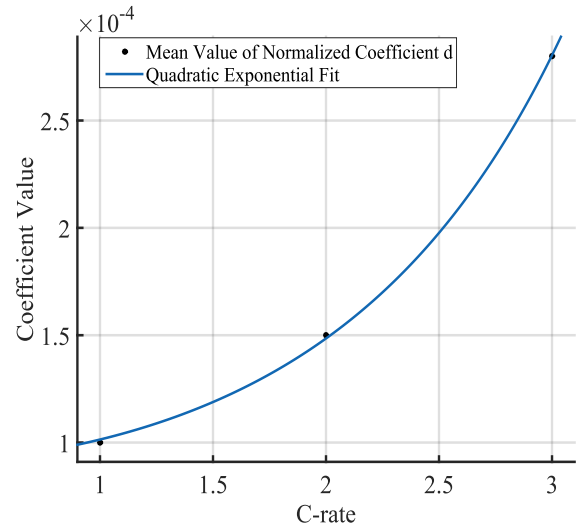

Figure 11. Quadratic exponential fit following the mean values of coefficient d.

Table 3. Alpha and beta values after adjusting the d coefficient through a quadratic exponential fit.

Parameter	α	β
Mean Value	8.93E-5	0.127
Confidence bounds	(6.94E-5, 1.09E-4)	(9.86E-2, 0.155)

Experimental Results

Characterization of the Panasonic CGR18650CH Li-ion Battery

To study the degradation process when cycling a Li-ion battery at high currents, a real experimental procedure was implemented. This procedure degraded a Panasonic CGR18650CH battery cell under controlled conditions for charge-discharge cycles and temperature (25°C). The procedure starts with a brand new battery cell as received from the manufacturer and consists of the following steps:

Charging Procedure

- The Constant Current Constant Voltage (CCCV) charge procedure should be done, firstly, at 0.5-C and this current must be applied until the voltage reaches 4.2 V. Then the voltage is fixed at this value and the current is reduced until it reaches 0.05-C.

Cycles 1-10: Initial cycles.

1. Perform discharge cycles at nominal current (1-C), (although the nominal current is defined at 2.25 A, for simplicity the experiments were done at 2.2 A).
2. Perform the CC-CV charging procedure.
3. Repeat steps 1-2 for ten cycles.

Cycles 11-12: Regular degradation cycles

1. Perform discharge cycles at 1-C.
2. Perform the CC-CV charging procedure.

Cycles 13-20: Accelerated degradation cycles

1. Perform discharge cycles at 2-C.
2. Perform the CC-CV charging procedure.

General considerations for all cycles

- A resting period of 30 minutes is established once the battery is discharged, and once the battery is charged.
- Cycles $10N + 11$ and $10N + 12$ $(N = 1, 2, 3, ...)$ shall be regular discharge cycles.
- All other cycles shall be accelerated degradation cycles.
- Repeat this alternating sequence of discharge process (two regular degradation cycles, and eight accelerated degradation cycles).
- The charging procedure must be undertaken after every discharge cycle, to start the new cycle with the battery fully charged.

The experiment started in November 2016 and finished in July 2017. Nearly 600 cycles were completed. Batteries were cycled in our laboratory using a Source Measuring Unit (SMU) (Keithley SourceMeter®). The software used for doing so uses a Coulomb counting method to register the battery capacity at each cycle. Figure 12 shows the degradation process for the normalized battery capacity. In this figure, it can be noted that two different trends co-exist. The uppermost set of points corresponds to discharges performed at 1-C, while the data points at the bottom correspond to cycles performed at 2-C.

An interesting situation happened between cycles 300 and 400. For unknown reasons the testing chamber stopped controlling the temperature, a fact that went unnoticed. Because of this fact, the amount of delivered energy decreased in those cycles. This effect has to be considered as a temperature-related phenomenon, and does not affect the degradation process in the long term. Indeed, once the issue with the testing chamber was fixed, degradation values came back to the expected trend.
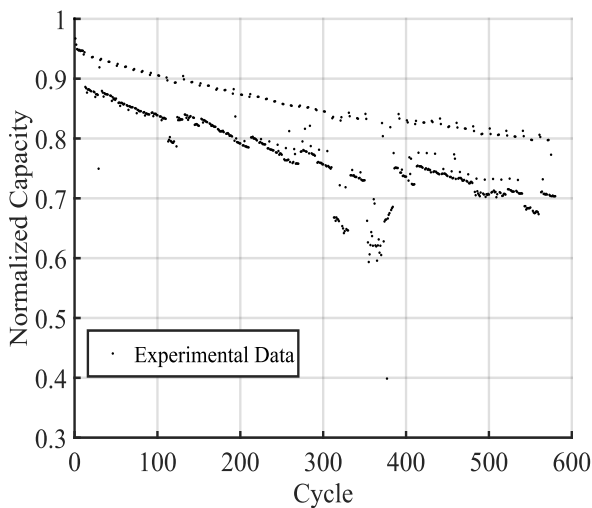

Figure 12. Experimental degradation process of the Panasonic CGR18650CH Li-ion battery.

Using the proposed model (Equations 1 and 2), fifty random realizations were generated and compared with the experimental data at both discharge current levels. Results are shown in Figure 13. Note that all model random realizations properly follow the trend of the experimental data. Without considering the experimental values that were

affected by the temperature problem, the difference between model realizations and the experimental data is less than 2%.
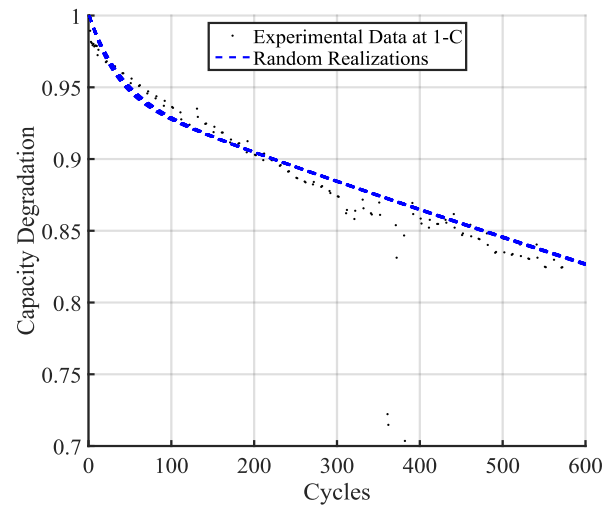

Figure 13. Comparison between experimental data at 1-C and fifty random realizations of the proposed model.

In this regard, it is possible to mention that the proposed model is able to properly characterize the degradation process for a given discharge current. The next step is to evaluate the performance of the model using the data results at 2-C. In a similar way, Figure 14 shows fifty random realizations of the proposed model and the experimental data.
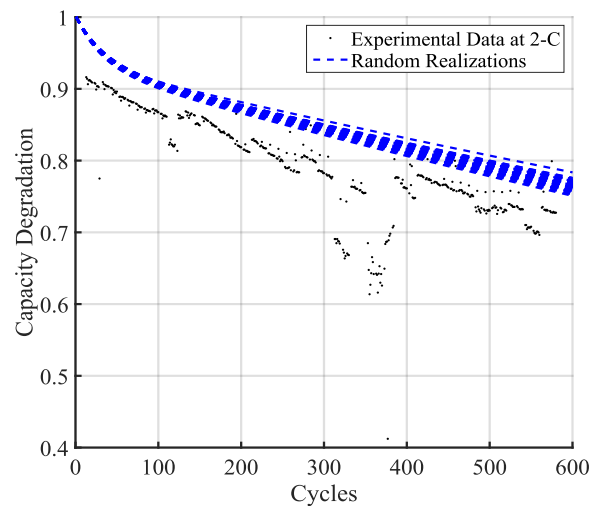

Figure 14. Comparison between experimental data at 2-C and fifty random realizations of the proposed model.

Figure 14 shows a bias between model realizations and measured data. However, an important fact to highlight is that the realizations follow the same trend as the experimental data, and that differences are between 5% and 7% in most cases. To verify this biased behavior, experimental data was fitted through the Curve Fitting Tool of Matlab®. To avoid the errors induced by low capacities due to the temperature-related phenomenon, these data points were excluded from the fitting process. Figure 15 shows the result when data is fitted by using the proposed model, and the confidence bounds for all the coefficients. Similarly to our previous

experiment, the resulting fitted curve follows the trend of the experimental data. The average offset is about 5%; and towards the end of the time series, the difference between the fitted values and the experimental data is limited to 3%. It is important to notice that various measured data points match the fitted curve.
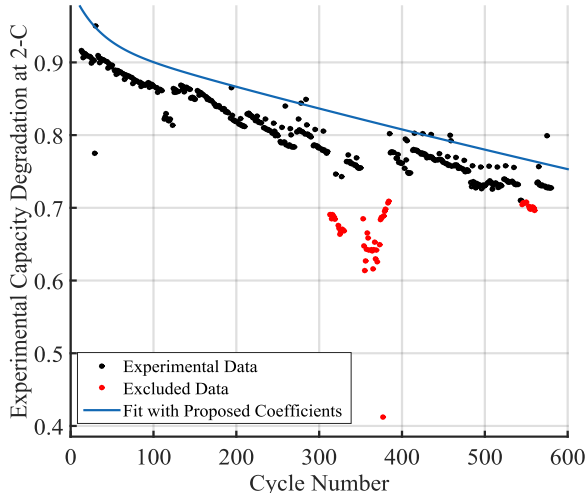

Figure 15. Fitted curve by using the proposed model and confidence bounds for all the coefficients.

To evaluate the model performance, we test the goodness of the fit (see Table 4). The statistics used for this purpose are: sum of squares due to error (SSE), the coefficient of determination (R^2), the adjusted coefficient of determination (Adjusted R^2), and the root mean squared error (RMSE). As expected, although the trend of the curve follows the experimental data, the results are not good enough. To overcome this situation, we have slightly modified the original parameter estimation procedure as follows.

Table 4. Goodness of the fit results for the experimental 2-C data.

Parameter	Value
SSE	0.7217
R^2	0.3982
Adjusted R^2	0.3997
RMSE	0.04237

As explained previously, the proposed model has two summands in observation Equation 2, which are parametrized by coefficients a and c. From those, coefficient c is the one that has the highest impact when characterizing the degradation process in the long term. In this regard, the coefficient c is left unbounded (or free) during the estimation process, while the feasible region for other coefficients is bounded within the confidence intervals shown in Table 1. Figure 16 shows the result of this special fit. Note how the bias is reduced just by setting the coefficient c free. For this new fit, the model is able to properly characterize the degradation process without the bias previously observed.

For the sake of comparison, the fitting procedure is repeated. In this case, though, the four coefficients are set free to let the Curve Fitting Tool of Matlab® adjust them; Figure 17 shows the results for this fit. As expected,
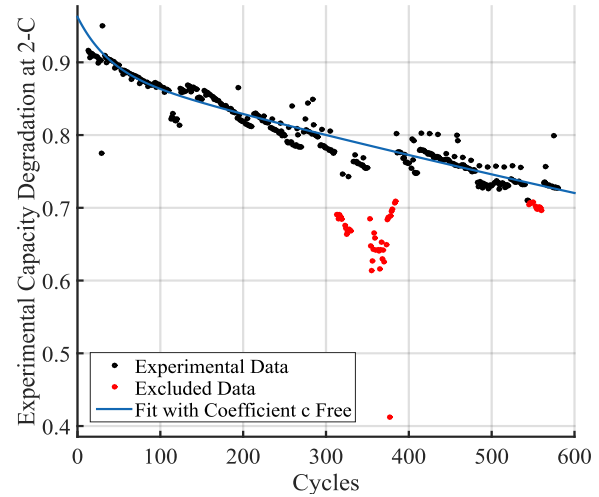

Figure 16. Fitted curve by setting coefficient c free.

the resulting fitted curve has a good performance when compared with the experimental data.
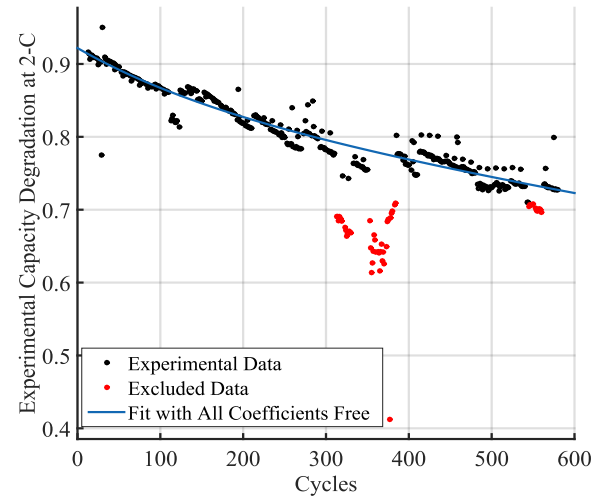

Figure 17. Fitted curve by setting all coefficients free.

A comparison between the goodness of both fits can be observed in Table 5. Expectedly, the results for the fit with free coefficients are better, although the results obtained where coefficient c is set free only are very similar.

Table 5. Comparison between the proposed model with coefficient c free only and all coefficients free.

Parameter	Coefficient c Free	All Coefficients Free
SSE	0.005995	0.0038
R^2	0.995	0.9968
Adjusted R^2	0.995	0.9968
RMSE	0.003866	0.00309

From these results, it is possible to state that the proposed model is able to properly fit the experimental data. Although using the obtained confidence bounds might induce a biased result, this does not mean that the model is not capable to properly represent the degradation process. For instance, the biased result can be amended if one of the coefficients is set

free. Although batteries are built under strict quality control conditions, due to the complex chemical processes involved, the degradation results may vary from cell to cell, especially when batteries are not used under nominal conditions. In this case, the model and the confidence bounds were obtained for a specific type of battery, and later applied on a different type of battery. As demonstrated, the proposed model is able to adjust the parameters in a simple and fast manner in order to characterize the observed process.

Sensitivity Analysis: Number of Samples Required for Model Parameter Estimation

Model parameter estimation was performed in our case using 300 measurements of battery capacity (one per cycle of operation). However, it is interesting to note that the proposed model structure allows to obtain accurate results using significantly less measurements. In this regard, we provide now a sensitivity analysis that will help to characterize the impact of smaller data sets in the resulting parameter estimates. In this sensitivity analysis, model coefficients, confidence intervals and prediction of the MSE were used to compare the characterization of the degradation process when using downsampled measurements of the battery capacity (i.e., when considering in the analysis one every five, ten or twenty measurements). Table 6 summarizes the obtained results. As expected, the lesser the measurements, the larger the confidence intervals for model parameters estimates (see Figure 18).

Table 6. RMSE for capacity degradation curves at three different discharge currents, when using different sampling periods.

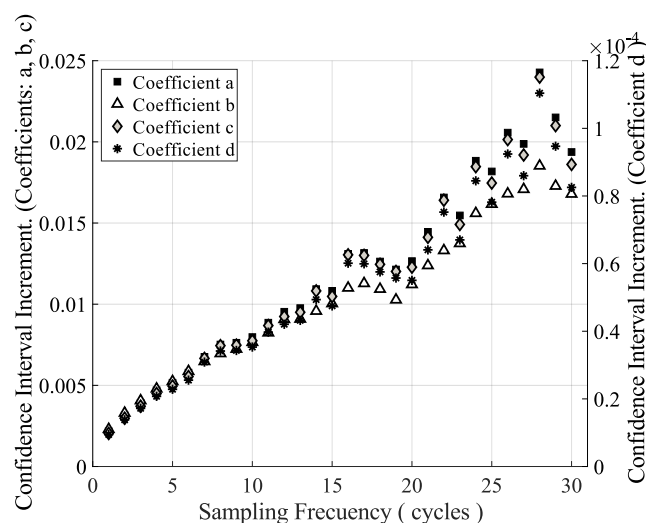| Sampling period (cycles)	1-C	2-C	3-C
1	0.00133	0.00387	0.00157
5	0.00135	0.00388	0.00158
10	0.00139	0.00392	0.00161
20	0.00149	0.00404	0.00169

Figure 18. Confidence interval increment as a function of the sampling period.

Hence, it can be determined that a minimum of 30 measurements (in our case, equivalent to use one every 10

available samples) are required to provide reasonably good estimates for the parameters of the proposed model structure.

Characterization of NASA Li-ion Battery Data Sets

One final case study is performed using two data sets obtained from the public repository of the Prognostics Center of Excellence of the NASA Ames Research Center. In this case, the data sets used are those associated with Batteries #34 and #36 (Available for download at https://ti.arc.nasa.gov/tech/dash/groups/pcoe/prognostic-data-repository/). In these experiments the room temperature was controlled at 24 degrees Celsius. The batteries have a nominal capacity of 2 Ah. Battery #34 was discharged at a constant current of 4 A until the discharge voltage reached 2.2 V at each cycle, while battery #36 was discharged at nominal current conditions until the discharge cycle reached 2.7 V at each cycle. The experiment was performed until the nominal capacity was reduced by 20% (i.e. from 100% to 80%).

Similar to the previous case study, the idea is to compare the proposed model under two conditions. The first condition is to set the confidence bounds for coefficients a, b, and d using the previously defined values. The second condition is to set coefficient c free and let the Curve Fitting Tool of Matlab® to adjust it. The first results shown in Figure 19 correspond to Battery #36. Note how the results where coefficient c is set free are able to properly fit the real data.
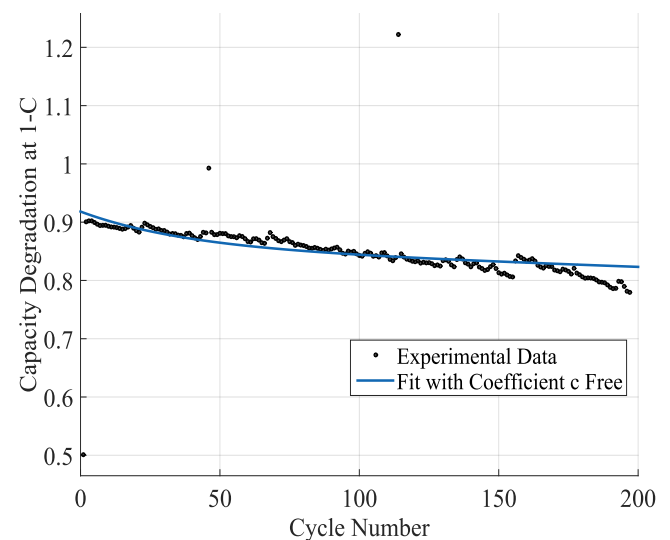

Figure 19. Fitted proposed model setting coefficient c free.

Figure 20 shows the results when all coefficients are set free. In this case the behavior of the fitted curve follows the trend of the data in a more precise manner, and there are no significant differences between the measured data and the fitted results.

Similarly to the previous case study, the goodness of the fit is analyzed. Table 7 shows the obtained results. Note that the differences among the four parameters are very small, and therefore the proposed model is also able to characterize the degradation process of this battery when discharged at nominal current.
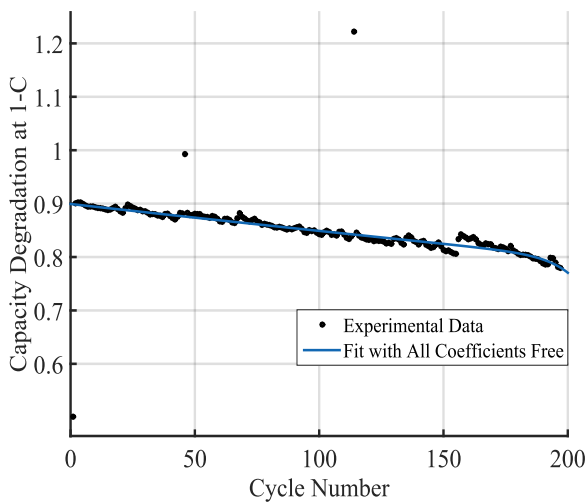
Figure 20. Fitted curve by using the proposed model setting all coefficients free.

Table 7. Comparison between the proposed model with coefficient c free only and all coefficients free applied on Battery #36.

Parameter	Coefficient c Free	All Coefficients Free
SSE	0.0279	0.02377
R^2	0.9397	0.9486
Adjusted R^2	0.9397	0.9478
RMSE	0.0119	0.0111

Next, the previous analysis is repeated on Battery #34. Figure 21 shows the result of the proposed model and confidence bounds except for those associated with coefficient c, which is set free, to be found by the software. Although the data looks irregular, the fitted result is capable to follow the trend.
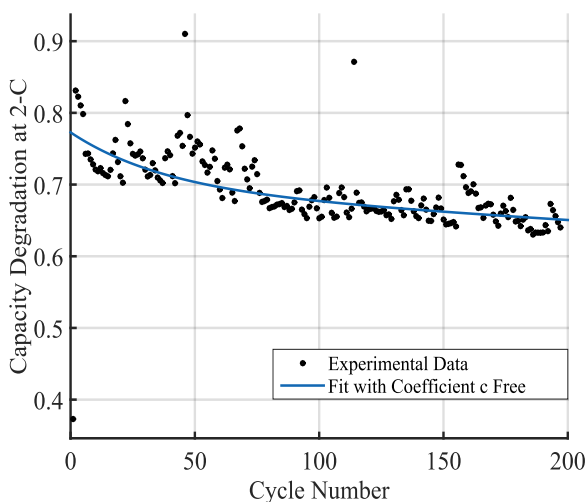

Figure 21. Fitted curve by using the proposed model setting coefficient c free.

Figure 22 shows the result where all coefficients are set free. In this case, it is more difficult to observe the differences between this and the previous result, since the measured data are more distributed.
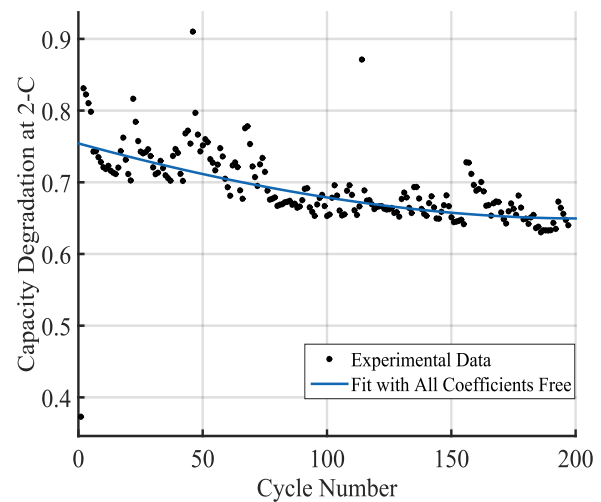

Figure 22. Fitted curve by using the proposed model setting all coefficients free.

Finally, both results are compared through the goodness of fit. Table 8 shows that the differences between both approaches are very small.

Table 8. Comparison between the proposed model with coefficient c free only and all coefficients free applied on Battery #34.

Parameter	Coefficient c Free	All Coefficients Free
SSE	0.02829	0.02584
R^2	0.946	0.9506
Adjusted R^2	0.946	0.9499
RMSE	0.01201	0.01157

Lifespan Analysis Using the Proposed Model

Following the proposed model structure, a Monte Carlo simulation was realized with the intention of determining how many cycles the battery can operate at different discharge rates until it reaches an 85% of its nominal capacity. As mentioned before this threshold is enough to consider the battery as degraded. Fifty thousand realizations were performed, and in each simulation nine hundred cycles were included. A randomly generated discharge current was assigned to each cycle, this way is possible to use the proposed model to characterize the degradation process when the battery was discharged at any of the following: 1-C, 2-C or 3-C. Figure 23 illustrates the degradation process for one realization. It is possible to note how the random realization at the beginning of the process has a similar behavior to the 1-C and 3-C trends, but after almost 50 cycles it begins to follow its own path. This is important since it is possible to quantify the amount of deliverable energy the battery has at the beginning of each cycle. Towards the end, the degradation process is more similar to the 2-C trend and crossing the 85% threshold almost at the same cycle.

To analyze the lifespan of the battery in terms of cycles, a histogram with the results of the realizations is shown in Figure 24. As seen, in this case the useful life of the battery can be characterized using a normal distribution, particularly N(400.39,128.09).
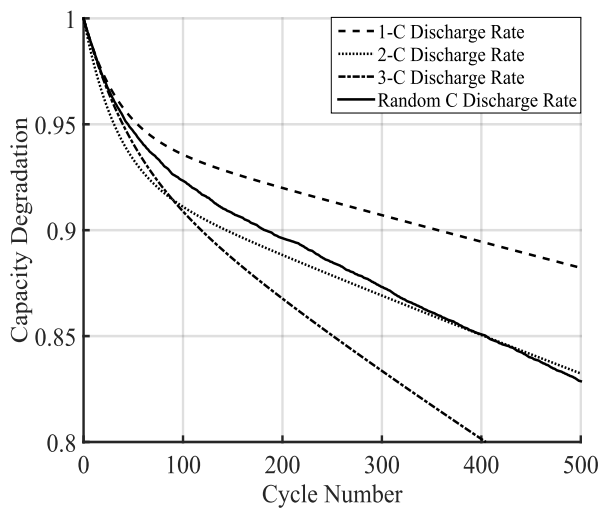
Figure 23. Illustrative example showing a Monte Carlo simulation for battery capacity degradation.
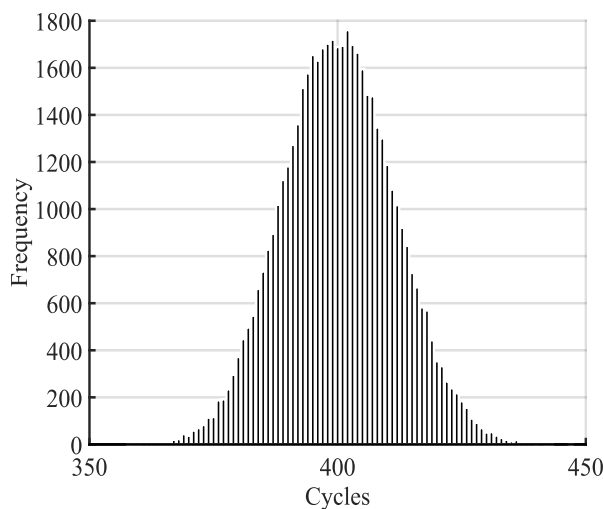

Figure 24. Cycle life of the battery when operated at random currents.

It is important to mention that if intermediate values of discharge currents are used, or perhaps different bounds, for example discharging the battery just between 1-C and 2-C, the cycle life will change.

Conclusions

This article proposes an empirical model that characterizes the degradation process of Li-ion batteries when discharged at various C-rates. The proposed model is based on a discrete state-space representation and uses two states and four coefficients, where one of the equations has a major impact on the short term degradation process, while the other affects the long term degradation. The proposed model can be adjusted to the discharge current used, demonstrating that one (out of four) coefficient presents a greater impact on the degradation process in the long term.

The proposed model and coefficient values can be easily and accurately adapted to different types of Li-ion batteries. This was validated under different discharge currents and two

sets of experimental data: our own experimental data set and those from the Prognostics Center of Excellence of NASA Ames Research Center.

One of the main advantages of the proposed model is that the current SOH can be calculated by evaluating a simple algebraic expression. Although using all the confidence intervals for the all the coefficients might induce a biased result, this can be amended by implementing a sequential learning method or other similar techniques to estimate coefficient c and we leave this for future research.

References

[1] Olivares B, Cerda M, Orchard M et al. Particle-filtering-based prognosis framework for energy storage devices with a statistical characterization of state-of-health regeneration phenomena. *IEEE Transactions on Instrumentation and Measurement* 2013; 62(2): 364–376.

[2] Awadallah MA and Venkatesh B. Accuracy improvement of soc estimation in lithium-ion batteries. *Journal of Energy Storage* 2016; 6: 95–104.

[3] Zahid T, Xu K and Li W. Machine learning an alternate technique to estimate the state of charge of energy storage devices. *Electronics Letters* 2017; 53(25): 1665–1666.

[4] El Mejdoubi A, Oukaour A, Chaoui H et al. State-of-charge and state-of-health lithium-ion batteries diagnosis according to surface temperature variation. *IEEE Transactions on Industrial Electronics* 2016; 63(4): 2391–2402.

[5] Wang D, Yang F, Zhao Y et al. Prognostics of lithium-ion batteries based on state space modeling with heterogeneous noise variances. *Microelectronics Reliability* 2017; .

[6] Perez A, Quintero V, Rozas H et al. Lithium-ion battery pack arrays for lifespan enhancement. In *2017 CHILEAN Conference on Electrical, Electronics Engineering, Information and Communication Technologies (CHILECON).* pp. 1–5. DOI:10.1109/CHILECON.2017.8229537.

[7] Jaguemont J, Nikolian A, Omar N et al. Development of a two-dimensional-thermal model of three battery chemistries. *IEEE Transactions on Energy Conversion* 2017; 32(4): 1447–1455.

[8] Vetter J, Novák P, Wagner MR et al. Ageing mechanisms in lithium-ion batteries. *Journal of Power Sources* 2005; 147(1-2): 269–281.

[9] Wong D, Wetz D, Mansour A et al. The influence of high c rate pulsed discharge on lithium-ion battery cell degradation. In *Pulsed Power Conference (PPC), 2015 IEEE*. IEEE, pp. 1–6.

[10] Daigle M and Kulkarni CS. Electrochemistry-based Battery Modeling for Prognostics. In *Annual Conference of the Prognostics and Health Management Society 2013*. PHM Society, pp. 1–13.

[11] Hirai T, Ohnishi A, Nagaoka N et al. Automatic equivalent-circuit estimation system for lithium-ion battery. In *2008 43rd International Universities Power Engineering Conference*. IEEE, pp. 1–5.

[12] Chen SX, Tseng KJ and Choi SS. Modeling of lithium-ion battery for energy storage system simulation. In *Power and Energy Engineering Conference, 2009. APPEEC 2009. Asia-Pacific*. IEEE, pp. 1–4.

[13] Rong P and Pedram M. An analytical model for predicting the remaining battery capacity of lithium-ion batteries. *IEEE Transactions on Very Large Scale Integration (VLSI) Systems* 2006; 14(5): 441–451.

[14] Pola D, Guajardo F, Jofré E et al. Particle-Filtering-Based State-of-Health Estimation and End-of-Life Prognosis for Lithium-Ion Batteries at Operation Temperature. In *Annual Conference of the Prognostics and Health Management Society 2016*. PHM Society, pp. 1–10.

[15] Rahimi-Eichi H, Ojha U, Baronti F et al. Battery management system: An overview of its application in the smart grid and electric vehicles. *IEEE Industrial Electronics Magazine* 2013; 7(2): 4–16.

[16] Berecibar M, Gandiaga I, Villarreal I et al. Critical review of state of health estimation methods of li-ion batteries for real applications. *Renewable and Sustainable Energy Reviews* 2016; 56: 572–587.

[17] Lotfi N, Li J, Landers R et al. Li-ion battery state of health estimation based on an improved single particle model. In *American Control Conference (ACC), 2017*. IEEE, pp. 86–91.

[18] Andre D, Appel C, Soczka-Guth T et al. Advanced mathematical methods of SOC and SOH estimation for lithium-ion batteries. *Journal of Power Sources* 2013; 224: 20–27.

[19] Haifeng D, Xuezhe W and Zechang S. A new SOH prediction concept for the power lithium-ion battery used on HEVs. In *Vehicle Power and Propulsion Conference, 2009. VPPC'09. IEEE*. IEEE, pp. 1649–1653.

[20] Ning G and Popov BN. Cycle Life Modeling of Lithium-Ion Batteries. *Journal of The Electrochemical Society* 2004; 151(10): A1584–A1591.

[21] Ning G, White RE and Popov BN. A generalized cycle life model of rechargeable Li-ion batteries. *Electrochimica Acta* 2006; 51(10): 2012–2022.

[22] Ning G, Haran B and Popov BN. Capacity fade study of lithium-ion batteries cycled at high discharge rates. *Journal of Power Sources* 2003; 117(1-2): 160–169.

[23] Saha B, Goebel K, Poll S et al. Prognostics Methods for Battery Health Monitoring Using a Bayesian Framework. *IEEE Transactions on Instrumentation and Measurement* 2009; 58(2): 291–296.

[24] Ng KS, Moo CS, Chen YP et al. Enhanced coulomb counting method for estimating state-of-charge and state-of-health of lithium-ion batteries. *Applied energy* 2009; 86(9): 1506–1511.

[25] Dalal M, Ma J and He D. Lithium-ion battery life prognostic health management system using particle filtering framework. *Proceedings of the Institution of Mechanical Engineers, Part O: Journal of Risk and Reliability* 2011; 225(1): 81–90.

[26] Yang F, Wang D, Xing Y et al. Prognostics of li(nimnco)o2-based lithium-ion batteries using a novel battery degradation model. *Microelectronics Reliability* 2017; 70: 70–78.

[27] Widodo A, Shim MC, Caesarendra W et al. Intelligent prognostics for battery health monitoring based on sample entropy. *Expert Systems with Applications* 2011; 38(9): 11763–11769.

[28] Williard N, He W, Osterman M et al. Comparative analysis of features for determining state of health in lithium-ion batteries. *International Journal of Prognostics and Health Management* 2013; 4: 1–7.

[29] Haiying W, Long H, Jianhua S et al. Study on correlation with SOH and EIS model of Li-ion battery. In *Proceedings of 2011 6th International Forum on Strategic Technology*, volume 1. IEEE, pp. 261–264.

[30] Le D and Tang X. Lithium-ion battery state of health estimation using Ah-V characterization. In *Annual Conference of the Prognostics and Health Management Society 2011*, volume 2. PHM Society, pp. 1–7.

[31] Eddahech A, Briat O and Vinassa JM. Real-time SOC and SOH estimation for EV Li-ion cell using online parameters identification. In *2012 IEEE Energy Conversion Congress and Exposition (ECCE)*. IEEE, pp. 4501–4505.

[32] He W, Williard N, Osterman M et al. Remaining useful performance analysis of batteries. In *2011 IEEE Conference on Prognostics and Health Management*. IEEE, pp. 1–6.

[33] Thirugnanam K, Saini H and Kumar P. Mathematical modeling of li-ion battery for charge/discharge rate and capacity fading characteristics using genetic algorithm approach. In *2012 IEEE Transportation Electrification Conference and Expo (ITEC)*. IEEE, pp. 1–6.

[34] Lam L and Bauer P. Practical capacity fading model for Li-ion battery cells in electric vehicles. *IEEE transactions on power electronics* 2013; 28(12): 5910–5918.

[35] Xie Y, Li J and Yuan C. Multiphysics modeling of lithium ion battery capacity fading process with solid-electrolyte interphase growth by elementary reaction kinetics. *Journal of Power Sources* 2014; 248: 172–179.

[36] Wang D, Yang F, Zhao Y et al. Battery remaining useful life prediction at different discharge rates. *Microelectronics Reliability* 2017; 78: 212–219.

Author Biographies

Dr. Aramis Perez received his B.Sc. degree and Licentiate degree in Electrical Engineering from the University of Costa Rica. He received his master degree in Business Administration with a General Management Major from the same university. He also received the Doctorate in Electrical Engineering degree from the

University of Chile. Currently he is a Research Fellow at the Energy Center of the Mathematical and Physical Sciences Faculty at the University of Chile and a Professor at the School of Electrical Engineering at the University of Costa Rica. His research interests include parametric/non-parametric modeling, system identification, data analysis, machine learning and manufacturing processes.

Vanessa Quintero received her B.Sc degree in Electronics and Telecommunication Engineering at the Universidad Tecnológica de Panamá (2007). Currently she is a doctorate student at the University of Chile. Her research interests include estimation, prognostics with applications to battery and protocols design.

Francisco Jaramillo received the B.Sc. degree in Electronics Engineering from Universidad de La Frontera, Temuco, Chile, in 2009. Currently he is a doctorate student at the Department of Electrical Engineering at the University of Chile under Dr. Marcos E. Orchard supervision. His research interests include machine learning, control systems, and estimation and prognosis based on Bayesian algorithms with applications to nitrogen removal in pilot-scale Sequencing Batch Reactors for Wastewater Treatment Plants.

Heraldo Rozas is a graduate student at the Department of Electrical Engineering at the University of Chile. His research interests include system identification, estimation theory and decision making under uncertainty.

Diego Jimenez received the Electronics and Instrumentation Engineering degree from University of the Armed Forces ESPE, Ecuador in 2014. He is currently pursuing the M.Sc. degree in Electrical Engineering at the University of Chile. His research interests include estimation, modularity in lithium-ion batteries and renewable energy.

Dr. Marcos E. Orchard received the B.S. degree and a Civil Industrial Engineering degree with electrical major from Catholic University of Chile. He also received the M.S. and Ph.D. degrees from The Georgia Institute of Technology, Atlanta, GA, USA. He is currently an Associate Professor with the Department of Electrical Engineering at the University of Chile. His current research interest is the design, implementation and testing of real-time frameworks for fault diagnosis and failure prognosis, with applications to battery management systems, mining industry, and finance.

Dr. Rodrigo Moreno received the B.Sc. and M.Sc. degrees from Catholic University of Chile and a Ph.D. degree from Imperial College London, U.K. He is currently an Assistant Professor at the University of Chile and a Research Associate at Imperial College London. His research interests are power systems optimization, reliability and economics, renewable energy, and the smart grid.